Received: 31 October 2020 | Revised: 15 January 2021 | Accepted: 18 January 2021

DOI: 10.1002/hyp.14063

RESEARCH ARTICLE

WILEY

# Spatiotemporal dynamics of water sources in a mountain river basin inferred through $\delta^2H$ and $\delta^{18}O$ of water

Lillian M. McGill[1] | J. Renée Brooks[2] | E. Ashley Steel[3]

[1]Quantitative Ecology and Resource Management, University of Washington, Seattle, Washington

[2]Pacific Ecological Systems Division, National Health and Environmental Effects Research Laboratory, U.S. Environmental Protection Agency, Corvallis, Oregon

[3]School of Aquatic and Fishery Sciences, University of Washington, Seattle, Washington

**Correspondence**
Lillian M. McGill, Quantitative Ecology and Resource Management, University of Washington, Seattle, WA 98105, USA.
Email: lmcgill@uw.edu

**Funding information**
Department of the Interior Northwest Climate Adaptation Science Center graduate fellowship; National Science Foundation Graduate Research Fellowship, Grant/Award Number: DGE-1762114

## Abstract

In mountainous river basins of the Pacific Northwest, climate models predict that winter warming will result in increased precipitation falling as rain and decreased snowpack. A detailed understanding of the spatial and temporal dynamics of water sources across river networks will help illuminate climate change impacts on river flow regimes. Because the stable isotopic composition of precipitation varies geographically, variation in surface water isotope ratios indicates the volume-weighted integration of upstream source water. We measured the stable isotope ratios of surface water samples collected in the Snoqualmie River basin in western Washington over June and September 2017 and the 2018 water year. We used ordinary least squares regression and geostatistical Spatial Stream Network models to relate surface water isotope ratios to mean watershed elevation (MWE) across seasons. Geologic and discharge data was integrated with water isotopes to create a conceptual model of streamflow generation for the Snoqualmie River. We found that surface water stable isotope ratios were lowest in the spring and highest in the dry, Mediterranean summer, but related strongly to MWE throughout the year. Low isotope ratios in spring reflect the input of snowmelt into high elevation tributaries. High summer isotope ratios suggest that groundwater is sourced from low elevation areas and recharged by winter precipitation. Overall, our results suggest that baseflow in the Snoqualmie River may be relatively resilient to predicted warming and subsequent changes to snowpack in the Pacific Northwest.

**KEYWORDS**
baseflow, climate, geology, spatial stream network models, water source, water stable isotopes

## 1 | INTRODUCTION

Climate change is projected to alter river hydrology across the Pacific Northwest. Within this region, the majority of precipitation occurs between October and March. Winter hydrology is therefore governed by the timing and form of precipitation, and summer hydrology is governed by snowpack melt and groundwater discharge. Seasonal asynchrony between precipitation largely occurring during winter and summer water demand makes water supplies scarce and vulnerable (Jaeger et al., 2013). Climate models predict an exacerbation of this vulnerability (Elsner et al., 2010; Hamlet et al., 2010). Substantial winter warming will lead to increased precipitation falling as rain, decreased amount and earlier onset of snowmelt, and increased evapotranspiration (Nolin & Daly, 2006; Stewart et al., 2005).

Pacific Northwest rivers with both significant winter rain and spring snowmelt, referred to as transient basins, are particularly climate sensitive and expected to experience substantial changes in the timing of runoff and streamflow (Vano et al., 2015; Wu et al., 2012). However, the impacts of climate induced changes to seasonal streamflow will be mediated by subsurface drainage processes that

  

translate water inputs into streamflow, such as the capacity for the landscape to retain and release precipitation as groundwater. Although several studies have predicted future streamflow based on climate mediated shifts in precipitation and snowpack regimes, few have highlighted the role of underlying geology in controlling hydrologic responses to climate change (Mayer & Naman, 2011; Safeeq et al., 2013; Tague & Grant, 2004, 2009). Furthermore, much of river management occurs at localized scales, and therefore demands an understanding of within basin spatial patterns of climate and geologic influence on streamflow processes. To identify streamflow vulnerability in a changing climate, approaches that take into account both climatic and geologic controls on water source are needed.

Previous approaches used to understand and assess climate risk have predominately relied on large, physically based runoff models coupled with general circulation models or statistical hydrologic classification schemes based on physical attributes or discharge metrics. Coupled climate-hydrology models have the benefit of simulating hydrologic processes under multiple climate scenarios and explicitly forecasting future hydrographs; however, many either do not explicitly simulate streamflow contributions from deep groundwater or approximate deep groundwater by extended soil profiles (Vano et al., 2010; Wenger et al., 2010). This can underestimate or inaccurately characterize groundwater contribution to streamflow and bias subsequent estimations of streamflow vulnerability (Safeeq, Mauger, et al., 2014). Statistical hydrologic classification approaches either classify locations according to attributes describing interactions of climate, geomorphology, and geology (Safeeq, Grant, et al., 2014; Tague & Grant, 2004; Wigington et al., 2013) or utilize emergent properties of discharge time series (Olden et al., 2011; Reidy Liermann et al., 2011; Wolock et al., 2004). Limitations of classification include poor data quality (e.g., soil and bedrock geology), incomplete understanding of hydrologic processes (e.g., groundwater–surface water connectivity), limited spatial coverage of stream gauges mostly restricted to large, downstream tributaries, and variable quality and quantity of discharge data available for each gauge (Kennard et al., 2009; Ruhi et al., 2018). Although physically based hydrology models and hydrologic classification provide a useful framework for expected streamflow behaviour and advance our ability to make predictions in unmonitored catchments, additional tools for understanding future streamflow will help address uncertainty around these approaches. For example, an understanding about spatial and temporal dynamics of where water originates in a basin will inform mechanisms of runoff generation and aid in predictions of where and how streamflow patterns are likely to shift.

A number of studies have used spatial variation in stable isotopes of input precipitation (Bowen et al., 2011) or in surface water across a basin (Brooks et al., 2012; Nickolas et al., 2017) to draw insights about variation in river water sources throughout the year. Water stable isotope ratios exhibit systematic spatial and temporal variation resulting from the process of isotope fractionation that accompanies water cycle phase changes and diffusion (Araguas-Araguas et al., 2000; Gat, 1996). An example of this process is the Rayleigh rainout effect, wherein progressive isotopic depletion of a vapour cloud occurs as it moves along its storm trajectory. Rayleigh rainout occurs because heavy isotopes preferentially fall as precipitation (Clark & Fritz, 1997; Dansgaard, 1964). As a result, both precipitation and surface water isotopic ratios of oxygen and hydrogen, expressed as $\delta^{18}O$ and $\delta^{2}H$, are highly correlated with changes in elevation, latitude, and longitude (Dutton et al., 2005; Ingraham & Taylor, 1991; Lechler & Niemi, 2011; Yonge et al., 1989), although the strength and presence of these relationships can vary among river basins due to local processes such as evaporation (Bowen & Good, 2015).

Previous work has shown that river water isotopes in windward basins draining the Cascade Range display a strong elevation gradient (Brooks et al., 2012; McGill et al., 2020). Here we explore how this elevation gradient can be used to understand how various portions of the watershed contribute to flow seasonally throughout a mid-size river basin and what the implications of source variation are for river flow dynamics in the future. We aim to understand potential watershed vulnerability to changes in precipitation type, timing, and location through understanding how water sources change seasonally and impact water supply across one river network. Specifically, our objective was to characterize spatial and temporal isotopic variation of surface waters within the Snoqualmie River, Washington to understand the vulnerability of river flow to source water dynamics across space and time. To complete this objective, we (1) measured and modelled surface isotope ratios across a network of sampling stations throughout the year, and (2) developed a conceptual framework of streamflow generation to understand how changing water storage reservoirs (e.g., snow and groundwater) contribute to streamflow.

## 2 | METHODS

### 2.1 | Study site

The Snoqualmie River drains a 1813 $km^2$ watershed on the west side of the Cascade Range, Washington (Figure 1). Major tributaries to the Snoqualmie River are the North Fork, Middle Fork, South Fork, Tolt River, and Raging River (Table 1). Headwaters lie primarily in forested public land. After the convergence of the North, Middle, and South Fork Rivers, the Snoqualmie River flows over Snoqualmie Falls then runs through a wide floodplain dominated by agricultural, residential, and commercial land use. The Snoqualmie River is home to ecologically and economically important runs of Coho, Chinook, pink, chum and steelhead salmon, including Endangered Species Act (ESA) listed Chinook and steelhead salmon. A dam and reservoir on the Tolt River provide approximately 30% of Seattle's drinking water.

The Snoqualmie River has a humid Mediterranean climate with dry summers and wet, mild winters influenced by its proximity to the Pacific Ocean (Figure 2). Precipitation occurs predominately from October to March. Precipitation isotope patterns were inferred from a 15-year record of precipitation isotopes collected in Corvallis, Oregon from 2003 to 2018 that represents the only available long-term precipitation stable isotope time series in a location with a similar climate to the Snoqualmie basin. Precipitation weighted means of weekly

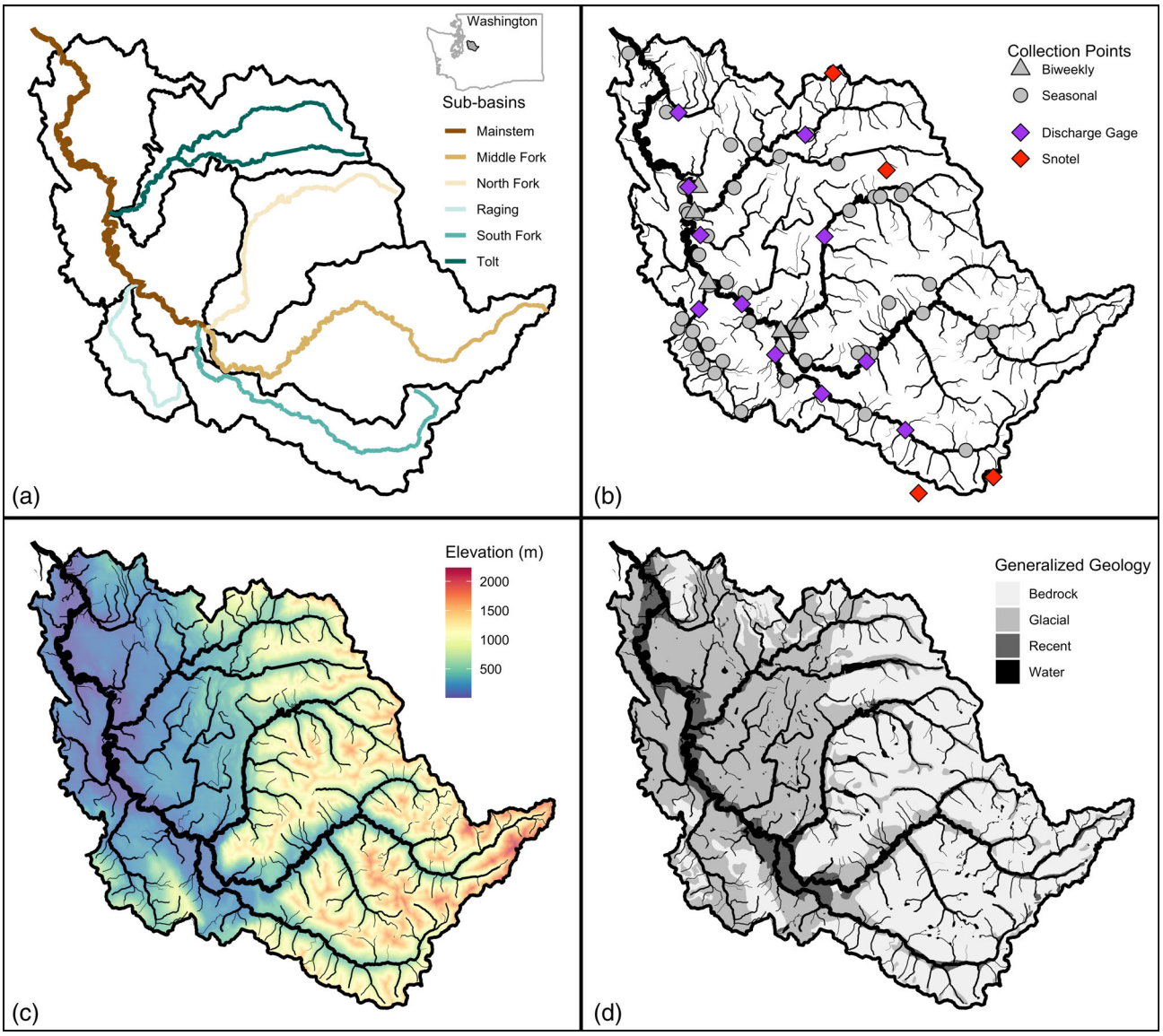


**FIGURE 1** The Snoqualmie River basin and sub-basins, and the Snoqualmie's location in Washington, USA (a), water sample, USGS gage, and SNOTEL site locations (b), elevation of the Snoqualmie basin (c), and generalized geology of the Snoqualmie basin (d)

**TABLE 1** Watershed characteristics for the Snoqualmie River and each of its major tributaries

| Subwatershed | Drainage area ($km^2$) | Mean watershed elevation (m) | Relief (m) | Mean annual precipitation (cm) | Mean slope (%) | Proportion of basin >900 m | Proportion of basin w/bedrock geology | Precip. weighted elevation (m) |
|---|---|---|---|---|---|---|---|---|
| Mainstem | 1781 | 637 | 2295 | 236 | 36.3 | 0.34 | 0.49 | 781 |
| Middle Fork | 442 | 988 | 2176 | 325 | 58.0 | 0.65 | 0.77 | 1043 |
| South Fork | 218 | 814 | 1771 | 267 | 44.1 | 0.46 | 0.65 | 890 |
| North Fork | 268 | 869 | 1667 | 281 | 47.9 | 0.53 | 0.71 | 919 |
| Tolt | 263 | 610 | 1801 | 217 | 33.9 | 0.25 | 0.46 | 710 |
| Raging | 84 | 442 | 1035 | 196 | 21.7 | 0.00 | 0.31 | 472 |

*Note*: The "snow zone" in the Snoqualmie is considered to be areas greater than 900 m (Jefferson, 2011). Mean annual precipitation was calculated over the period 1980–2010.

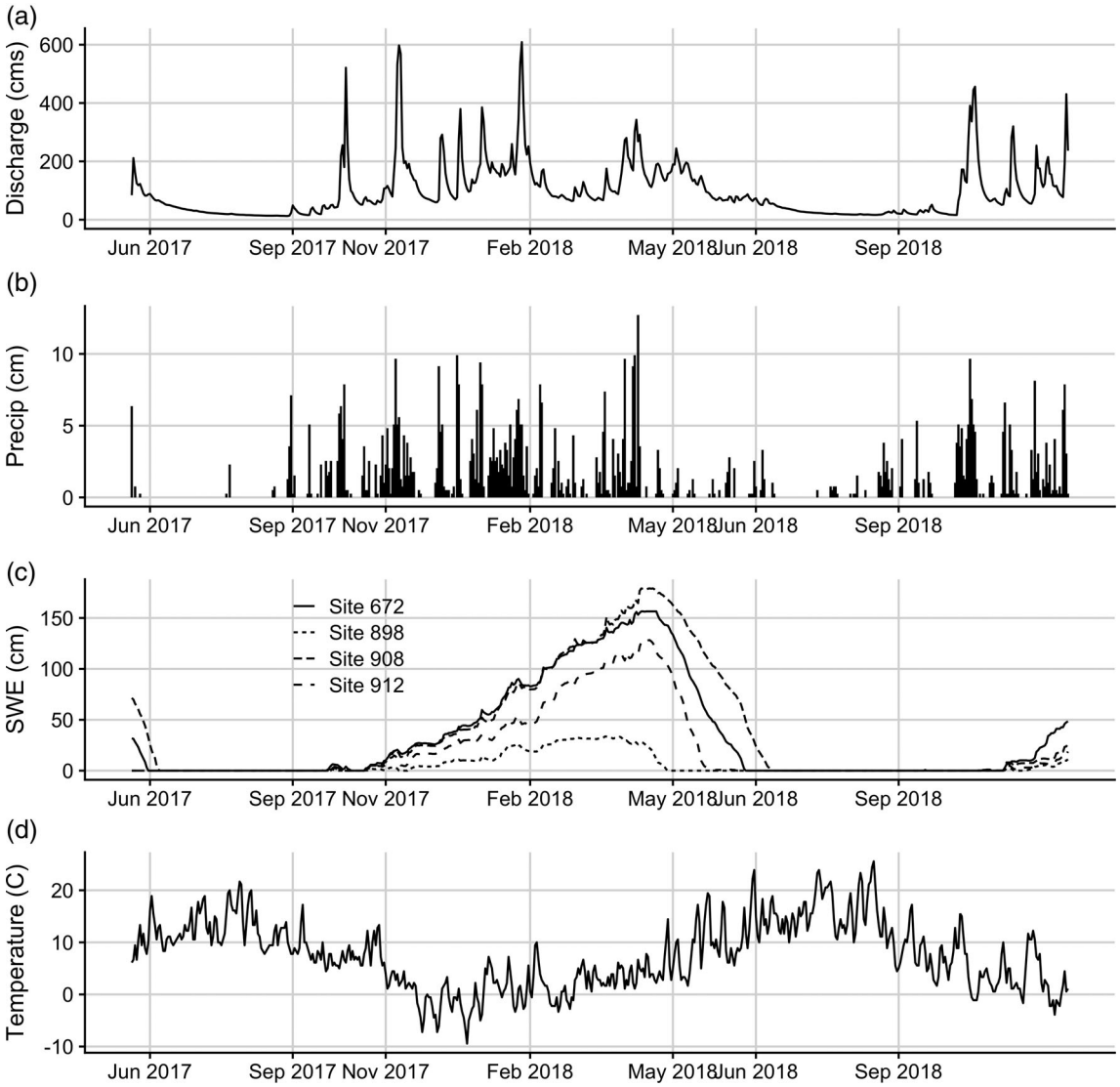


**FIGURE 2** Climatic time series over our study period. Mainstem Snoqualmie River discharge from USGS station 12149000 (a), total daily incoming precipitation from SNOTEL site 908 (b), snow-water-equivalent (SWE) from all SNOTEL sites within the basin (c), and mean daily air temperature from SNOTEL site 908 (d). The ticks on the x-axis are the median date of our whole basin, seasonal sampling events

precipitation isotopes do not show evidence of variation with season (ANOVA $p > 0.1$), although summer precipitation values are characterized by the lowest values of d-excess. The coldest month is typically January, whereas the warmest is July. The Snoqualmie River has a mixed rain-snow hydrology, with both substantial winter rain and spring snowmelt. The strong elevational temperature gradient controls the phase of precipitation. Areas of the basin below 300 m receive winter rain, while seasonal snow accumulates in areas above 900 m (Jefferson, 2011). Intermediate elevations (300–900 m) are occupied by a transient snow zone, where snow falls and melts more than once per winter (Table 1).

Geology of the Snoqualmie River basin includes parts of two major physiographic provinces: the Puget Lowland and the Middle Cascade Range (Buffington et al., 2003; Figure 1). In the lowland portion of the watershed, geology and topography are primarily products of repeated continental glaciations. Glacial and interglacial deposits underlay the Snoqualmie and Tolt Valleys (Bethel, 2004). In the alpine area, much of the ground surface is directly underlain by bedrock, and the bedrock units do not contain significant fracture systems (Bethel, 2004; Debose & Klungland, 1983; Goldin, 1973, 1992; Nelson, 1971; Turney et al., 1995).

## 2.2 | Data collection

We collected water samples across 49 sites within the Snoqualmie River basin during June 2017, September 2017, November 2017, February 2018, May 2018, June 2018 and September 2018 for a total of 364 samples (Figure 1). Sampling dates represent five major hydrologic periods: fall wet-up (November), winter wet period (February),

spring snowmelt (May), early summer (June), and summer lowflow (September). Sampling sites within the basin were selected to include a mix of mainstem and tributary locations and to span the elevation range found within the basin. We also collected biweekly water samples at the outlet of each major tributary and the Snoqualmie mainstem for a total of 181 samples (Figure 1). Sampling sites were selected to coincide with a long-term water temperature monitoring program described in Steel et al. (2016). Seasonal samples were collected to understand basin-scale patterns in isotope ratios throughout the year whereas biweekly samples were collected to understand fine scale temporal patterns of source water change within each major tributary. Water samples were collected within wading distance from the stream edge, but in flowing current. Samples were collected in 20 mL vials with conical plastic cap inserts to prevent evaporation, and duplicates were collected for every 20th sample.

Water isotopes analysis was performed on a Laser Absorption Water-Vapour Isotope Spectrometer (Model 908-0004, Los Gatos Research, Mountain View, CA) located at the Integrated Stable Isotope Research Facility at the Pacific Ecosystems Systems Division of the Environmental Protection Agency, Corvallis, Oregon. Samples were run under high precision analysis mode using a 10 μl syringe for a total of six injections per sample, with the first three discarded to eliminate memory effects. All $\delta^2$H and $\delta^{18}$O values were expressed relative to Vienna-Standard Mean Ocean Water (V-SMOW) using $\delta$ notation:

$$\delta^2 H \text{ or } \delta^{18}O = \frac{R_{sample}}{R_{standard}} - 1,$$

where $R$ is the ratio of $^2$H to $^1$H atoms or $^{18}$O to $^{16}$O atoms and the standard V-SMOW. Values were reported in parts per thousand (‰) by multiplying by 1000. Samples were calibrated to the VSMOW-SLAP scale using three laboratory standards spanning the range of sample values and calibrated annually to the IAEA certified standards. In addition, a separate QC standard was used to independently check the calibration and determine accuracy. Accuracy was 0.06 ± 0.11‰ for $\delta^{18}$O and 0.1 ± 0.27‰ for $\delta^2$H over the sample sets analyzed for this study. Measurement precision estimates (±1 standard deviation) were determined on repeated measures of both field and lab duplicates and were 0.11‰ for $\delta^{18}$O and 0.25‰ for $\delta^2$H. Samples that experienced significant evaporation prior to sample collection (e.g., water impounded by beaver ponds) may not reflect the spatial pattern of input precipitation and so were removed from analysis. Based on d-excess variance in Corvallis precipitation isotope data, we removed 14 samples with d-excess values below 5‰, all in low gradient rivers sampled in spring and summer.

Watersheds for each sampling point were delineated and landscape variables describing the watersheds were derived from commonly available geostatistical products. Watershed area and mean watershed elevation (MWE), watershed relief, and proportion of area above 900 m were calculated using the National Elevation Dataset, a 30-m resolution digital elevation model (Gesch et al., 2018). Mean watershed 30-year average mean annual precipitation (MAP) and precipitation weighted mean elevation for the period 1981–2010 were calculated (Hill et al., 2015). Geologic information was collected from the Washington DNR Division of Geology and Earth Resources (Frizzell et al., 1984; Tabor et al., 1993; Yount & Gower, 1991). Detailed lithology of the Snoqualmie basin was summarized into three major groups, bedrock, glacial, and recent lithology, based on the classification scheme of Bethel (2004). Precipitation, snow water equivalent (SWE), and air temperature were collected from four Snowpack Telemetry (SNOTEL) stations within or extremely close to the Snoqualmie basin (USDA Natural Resources Conservation Service, 2020). We obtained daily annual streamflow data from the U.S. Geologic Survey (USGS, 2001) and the King County Hydrologic Information Center for 11 sites within the Snoqualmie basin having data for the 2017 and 2018 water year (Figure 1).

## 2.3 | Analysis

Two modelling approaches were used to understand how the relationship between MWE and stream water isotope ratios varied through time. We first used ordinary least squares regression to fit a linear model with MWE to $\delta^{18}$O and $\delta^2$H for each month separately, and then with month as a factor to determine if slopes were statistically different from one another. Slopes, intercepts, and $R^2$ values were compared among models. We further modelled the spatial relationship between $\delta^2$H and MWE using a class of geostatistical models, spatial stream network models (SSNMs), which account for spatial dependencies across stream networks (Ver Hoef & Peterson, 2010). As $\delta^{18}$O and $\delta^2$H values are highly correlated (Clark & Fritz, 1997), SSNM regression analyses considered only $\delta^2$H values. SSNMs are similar to conventional linear mixed models in that the deterministic mean of the dependent variable is modelled as a linear function of explanatory variables; however, the assumption of independent errors is relaxed and an autocovariance model is used to account for spatial autocorrelation in the errors (Peterson & Ver Hoef, 2010; Ver Hoef et al., 2006; Ver Hoef & Peterson, 2010). We compared slopes and variance decomposition results from these SSNMs.

We also visualized spatial autocorrelation in model residuals using semivariograms. Semivariograms depict how semivariance, or average variation between measurement values separated by some distance, changes in relation to the distance separating them. Low semivariance values indicate that sample pairs within some distance are similar, whereas high values indicate dissimilar sample pairs. We displayed and compared two measures of distance between points: flow-connected distance (a network-based measure) and Euclidean distance (a straight-line measure). Semivariance was calculated using the robust estimator (Cressie, 1993). We estimated the semivariogram at lag distances whose bins contained greater than 10 site-pairs and that were less than half the maximum flow-connected distance between sites (Zimmerman & Ver Hoef, 2017). We examined semivariograms to visualize dependencies in residuals from linear models that include MWE as a covariate. Semivariograms

were compared to one another to identify scales of spatial autocorrelation (Brennan et al., 2016; McGuire et al., 2014).

We also examined the relationship between streamflow, geology, and water source. For each streamflow gaging station, we calculated two streamflow statistics based on the period of record to characterize individual stream hydrology: unit discharge at baseflow and baseflow index. Unit discharge at baseflow, or specific discharge, was calculated by dividing average streamflow for the month of September by the upstream contributing area for each gage location (Floriancic et al., 2019; Tague & Grant, 2004). Baseflow index is the ratio of annual baseflow to total streamflow and it represents the contribution of groundwater to river flow (Beck et al., 2013; Smakhtin, 2001). Baseflow unit discharge and baseflow index were calculated for both the 2017 and 2018 water years. For each streamflow gaging station, we also identified the seasonal isotope sampling location closest to each site and calculated two isotope statistics to characterize water source: water source variability and baseflow isotope value. Water source variability is the standard deviation of all $\delta^2H$ values from a site and reflects how water sources shift throughout the year ($\delta^2H_{SD}$). Baseflow isotope value is simply the September $\delta^2H$ value from a site, which varies with the mean elevation of source water at that time and place. Water source variability was calculated as one value across our sampling period, whereas the baseflow isotope value was calculated separately for September 2017 and 2018. We examined the relationship between baseflow index and water source variability and baseflow unit discharge and baseflow isotope value and the relationships between generalized geology, unit discharge, and baseflow index for each gage site.

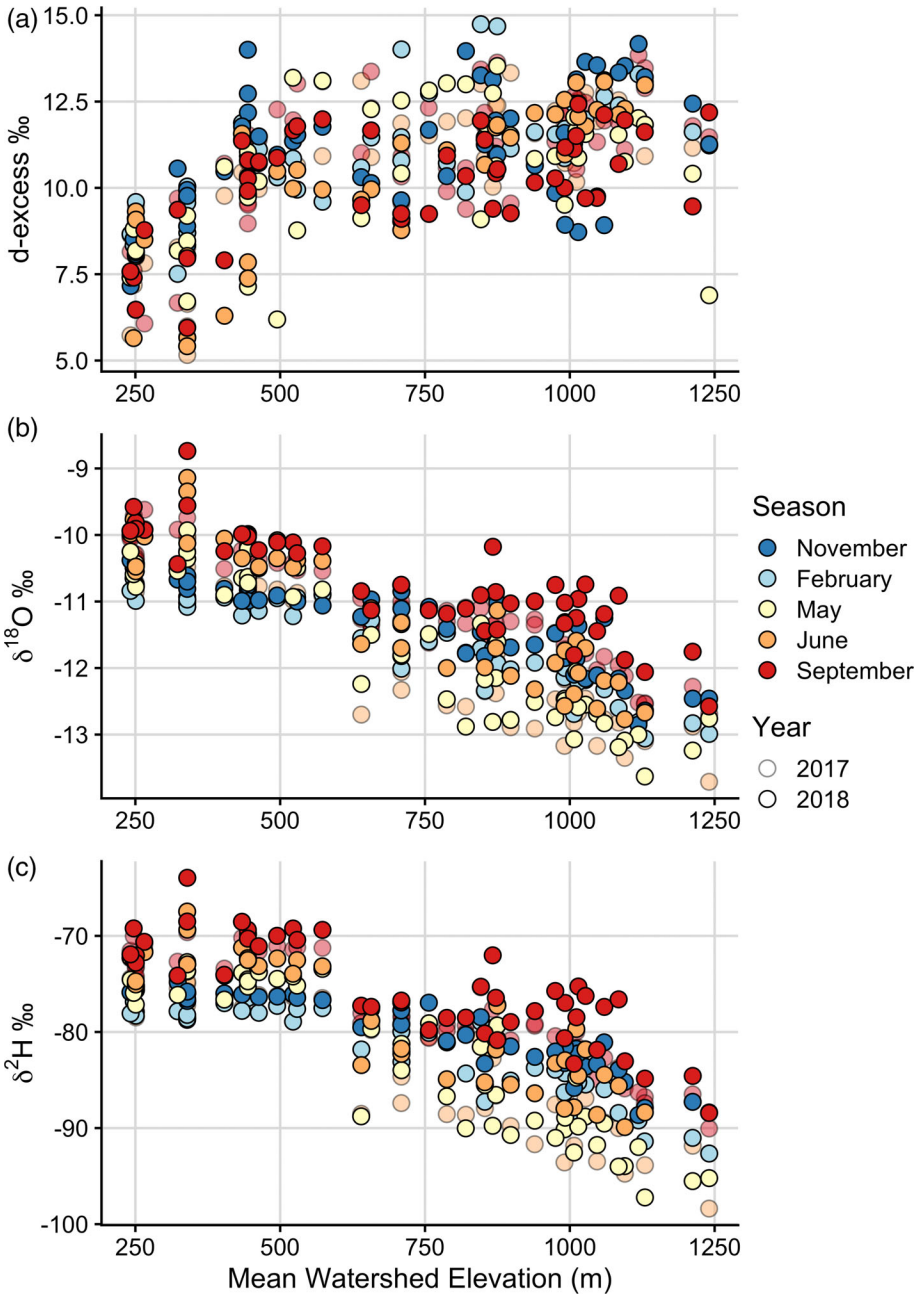


**FIGURE 3** Relationships with MWE for d-excess (a), $\delta^{18}O$ values (b), and $\delta^2H$ values, (c) for all seasonal sampling events. Colour indicates the month that each water sample was collected. For September and June, there are two sets of sampling events shown (2017 and 2018), with 2017 having a faded colour

All data analyses were conducted in R (http://cran.r-project.org) using the Spatial Stream Network (SSN) and lfstat packages (Koffler et al., 2013; Ver Hoef et al., 2014) and the Spatial Tools for the Analysis of River Systems (STARS) toolbox in ArcGIS 10.6 (Peterson & Ver Hoef, 2014).

## 3 | RESULTS

### 3.1 | General patterns in isotope ratios

Drainage areas of seasonal sampling sites ranged in size from 3–1780 $km^2$. Surface water isotope ratios for all seasonal samples within the Snoqualmie ranged from −13.7 to −8.7‰ for $\delta^{18}O$ and from −98.4 to −63.9‰ for $\delta^2H$ over the sampling period (Figure 3).

Samples with d-excess values substantially below 10‰ have been likely influenced by evaporation since falling as precipitation. Most surface water samples fell on the Global Meteoric Water Line (GMWL) indicating no evaporative influence (Figure S1). D-excess values ranged from −3.75 to 14.74‰ over the course of the year. Low elevation sites, such as those found in the Raging, Tolt, and Mainstem Snoqualmie tended to have the lowest d-excess values, regardless of season (Figure 3).

### 3.2 | Relationships between isotope ratios and MWE

$\delta^{18}O$ and $\delta^2H$ values of water decreased linearly with MWE, although the strength of the relationship is stronger for $\delta^{18}O$. $R^2$ values from regressions of seasonal samples for individual months range from 0.77 to 0.87 for $\delta^{18}O$ and from 0.71 to 0.82 for $\delta^2H$ (Figure 3; Table 2). When all months were considered simultaneously, $R^2$ values were 0.73 for $\delta^{18}O$ and 0.65 for $\delta^2H$. $R^2$ values increased to 0.83 for $\delta^{18}O$ and 0.77 for $\delta^2H$ when month was included as a factor in the linear regression because slopes varied significantly among months.

The relationship between MWE and isotope ratios changed through time (Figure 3). Slopes for isotope-MWE relationships were smallest in November (−1.9‰ $km^{-1}$, −11‰ $km^{-1}$) and February (−2.1‰ $km^{-1}$, −13‰ $km^{-1}$; Table 2) for $\delta^{18}O$ and $\delta^2H$, respectively. Slopes in May (−3.3‰ $km^{-1}$, −22‰ $km^{-1}$) and June (−2.8‰ $km^{-1}$, −17‰ $km^{-1}$) were the largest for $\delta^{18}O$ and $\delta^2H$, respectively. Slopes for $\delta^{18}O$ and $\delta^2H$ in September were intermediate (−2.3‰ $km^{-1}$, −14‰ $km^{-1}$). Sites below 550 m had little relationship between MWE and isotope ratios. We did not observe any clear seasonal variation in d-excess (Figure 3).

To examine how spatial autocorrelation impacted the relationship between MWE and isotope ratios, we compared model fit and variance decomposition for SSNMs for $\delta^2H$ isotope ratios for each month. Proportion of variation explained by spatial structure is fairly consistent among months, ranging from 15–30%. All SSNMs had better predictive ability than non-spatial models, with $R^2$ values ranging from 0.86 to 0.94 (Table 3).

Spatial dependencies within the Snoqualmie basin varied with month for $\delta^2H$ residuals after accounting for effects of MWE (Figure 4). For the Snoqualmie basin residual $\delta^2H$ values, semivariance for Euclidean distance (i.e., the straight line distance between all sites) and for flow-connected sites (i.e., the network distance between sites that share flow) increased rapidly and linearly before levelling off around 10 km for May 2018 and June 2017 and 2018 and around 25 km for September 2018. This change in semivariance suggests that residuals from sites beyond 10 or 25 km apart were uncorrelated, whereas residuals from sites closer together were more highly correlated with one another after accounting for effects of MWE. November 2018, February 2018, and September 2017 overall had much smaller semivariance values that do not observably level off indicating that basin $\delta^2H$ residuals are overall more similar.

### 3.3 | Seasonal variance in isotope ratios

Surface water isotope ratios varied seasonally in all surface water sampling sites, but low elevation (LE) sites (below 550 m) and high elevation (HE) sites (above 550 m) had distinctly different patterns (Figure 5). For both LE and HE sites, isotope values were highest in September ($\delta^2H_{LE}$ = −70.3 ± 1.2‰, $\delta^2H_{HE}$ = −78.6 ± 3.9‰) at the end of the long dry summers. Isotope ratios declined with winter precipitation inputs and were lowest at LE sites in February

**TABLE 2** Model fit statistics from linear regressions with mean watershed elevation (MWE) in the Snoqualmie River basin

| | $\delta^{18}O$ | | | $\delta^2H$ | | |
|---|---|---|---|---|---|---|
| | $R^2$ | Coefficient (SE) | Intercept (SE) | $R^2$ | Coefficient (SE) | Intercept (SE) |
| November (*n* = 48) | 0.81 | −0.0019 (0.00019) | −9.98 (0.14) | 0.81 | −0.011 (0.0011) | −71.74 (0.81) |
| February (*n* = 45) | 0.87 | −0.0021 (0.00014) | −10.16 (0.099) | 0.77 | −0.013 (0.0012) | −73.03 (0.84) |
| May (*n* = 47) | 0.84 | −0.0033 (0.00026) | −9.26 (0.19) | 0.82 | −0.022 (0.0021) | −66.26 (1.56) |
| June (*n* = 90) | 0.83 | −0.0028 (0.00018) | −9.29 (0.13) | 0.78 | −0.017 (0.0014) | −68.10 (0.96) |
| September (*n* = 92) | 0.77 | −0.0023 (0.00018) | −9.24 (0.13) | 0.71 | −0.014 (0.0013) | −66.05 (0.96) |
| All months | 0.73 | −0.0025 (0.00012) | −9.50 (0.82) | 0.65 | −0.015 (0.00088) | −68.49 (0.63) |
| All months (with month as a factor) | 0.83 | −0.0025 (0.000095) | −9.95 (0.10) | 0.77 | −0.015 (0.00071) | −71.15 (0.79) |

*Note*: Units for the coefficients are ‰/m. Numbers in parentheses are the standard error (SE) for model parameters.

**TABLE 3** Spatial stream network model (SSNM) statistics for each month

| | $\delta^2H$ | | | | |
|---|---|---|---|---|---|
| | | | | Variance component | |
| | $R^2$ | Coefficient (SE) | RMSPE | Fixed (%) | Spatial (%) |
| November ($n$ = 48) | 0.93 | −0.019 (0.0016) | 1.04 | 72 | 21 |
| February ($n$ = 45) | 0.93 | −0.013 (0.0013) | 1.16 | 72 | 21 |
| May ($n$ = 47) | 0.89 | −0.016 (0.0018) | 2.57 | 69 | 20 |
| June 2017 ($n$ = 48) | 0.94 | −0.021 (0.0015) | 1.64 | 74 | 20 |
| June 2018 ($n$ = 42) | 0.91 | −0.013 (0.0011) | 1.91 | 69 | 22 |
| September 2017 ($n$ = 46) | 0.94 | −0.021 (0.0021) | 1.29 | 79 | 15 |
| September 2018 ($n$ = 46) | 0.86 | −0.013 (0.0017) | 1.93 | 56 | 30 |

*Note:* All sites were included in these regressions. Units for the coefficients are ‰/m.

($\delta^2H_{LE}$ = −77.7 ± 0.8‰). However, HE sites continued to decline and were lowest in May ($\delta^2H_{HE}$ = −87.9 ± 5.7‰), while LE isotopic values increased in May causing May to have the greatest variability observed across sites. By June, isotopic ratios at all sites had increased.

Outlets of major tributaries and the mainstem sampled biweekly show similar seasonal patterns (Figure 6). Sites with a substantial proportion of the basin above 900 m (Table 1), including the Mainstem, North Fork, Middle Fork, and South Fork, showed a decrease in isotope ratios beginning in late April through May. Although little precipitation occurred after May, discharge remains relatively high, as compared to the low elevation tributary (Raging). The drop in isotopic ratios and sustained flow in these tributaries likely reflects the input of snowmelt. For all sites except the regulated Tolt, isotope ratios increase throughout the summer as flow drops to its lowest annual value and with little new precipitation falling. The increase began in January for the Raging and in May after the spring freshet for the Mainstem, North Fork, Middle Fork, and South Fork. In addition to broad seasonal patterns, two basin-wide shifts in surface water isotope ratios occurred during storm events. The first occurred on December 30th, 2017 and resulted in a decrease in isotope ratios ranging from 3.1–6.2‰. The second occurred on November 6th, 2018 and resulted in an increase in isotope ratios ranging from 3.3–10.5‰ compared to the previous sampling event.

### 3.4 | Relationships between discharge and geology

Baseflow index for all sites ranged from 0.43–0.98 with a mean of 0.63 and unit discharge at baseflow ranged from 0.03–0.70 $m^3\ s^{-1}\ km^{-2}$ with a mean of 0.36 $m^3\ s^{-1}\ km^{-2}$. $\delta^2H_{SD}$, for example, water source variability, ranged from 0.50–6.54‰ with a mean of 3.50‰. September 2017 and 2018 $\delta^2H$ values ranged from −84.91 to −69.77‰ with a mean of −77.39‰.

Unit discharge at baseflow increased positively and linearly with $\delta^2H$ values; however, two separate groups with similar patterns emerged (Figure 7a). Watersheds with a mean elevation above 550 m generally increase unit baseflow with increasing baseflow isotopic values up to −75‰ indicating more lower elevation water leads to greater baseflow. However, three relatively small watersheds with mean elevations lower than 550 m fall in a separate line with much lower unit discharge values (0.04–0.16 $m^3 s^{-1}\ km^{-2}$). Within these low elevation basins, baseflow unit discharge also increases with higher water isotope values.

Baseflow index was not related to water source variability (Figure 7b). The two sites with the lowest water source variability have the largest baseflow index, however the remaining sites are clustered between baseflow index values of 0.43–0.69 and display no relationship with water source variability.

Generally, baseflow index increases linearly with the proportion of low elevation glacial deposits underlying the catchment (Figure 8). A notable exception to this is the Raging, which is underlain by a large percentage of glacial deposits (69%) but has a low baseflow index ($BFI_{2017}$ = 0.48, $BFI_{2018}$ = 0.43). The relationship between the proportion of glacial deposits and unit discharge is less clear (Figure 8). Streams underlain by a higher proportion of glacial deposits do not necessarily have a higher unit discharge at baseflow. Notably, all streams with greater than 50% of their catchment underlain by glacial deposits, including the Raging and two additional low elevation tributaries, have very low unit discharge.

## 4 | DISCUSSION

### 4.1 | Isotope ratios vary strongly with MWE

Surface water isotopes in the Snoqualmie basin primarily varied with MWE (Figure 3). The strong observed elevation gradient can be attributed to the rainout effect, or Rayleigh distillation (Clark & Fritz, 1997; Dansgaard, 1964). Storms bringing precipitation to western Washington basins originate from the Pacific Ocean and move eastward. Continued rainout as storms move inland and up the Cascade Mountains produces $^{18}O$ and $^{2}H$ depleted precipitation at higher elevations. Close proximity to the Pacific Ocean exacerbates the rainout process. As the warm, wet air mass travels up the Cascade Mountains, it experiences orographic lifting and adiabatic cooling, resulting in increased precipitation strengthening the observed isotopic trends

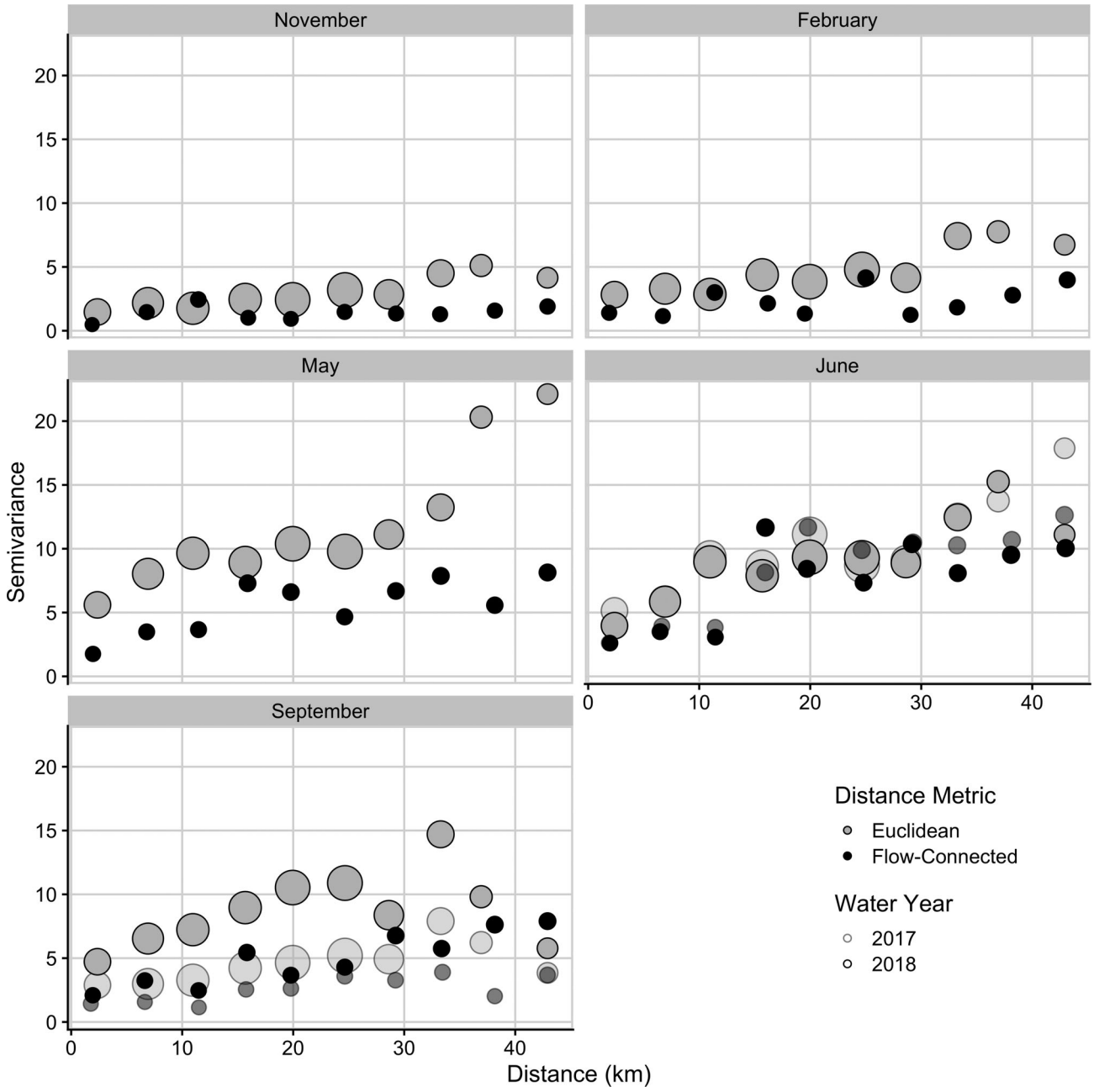


**FIGURE 4** Semivariograms for the residuals from the $\delta^2$H-MWE linear regression. Circles are proportional to the number of sites used to estimate each bin value

with elevation. Results are consistent with previous studies, which found that in coastal proximal settings precipitation $\delta^2$H variability follows an open-system behaviour in which precipitation is not recycled by evaporation, and the isotopic fractionation is compatible with a Rayleigh distillation process as the air rises and cools over mountains (Ingraham & Taylor, 1986, 1991). In surface water samples, studies across western Washington river basins have found that MWE is the dominant predictor of isotope ratios, but basin scale factors such as geology, geographic location, and landscape attribute configuration can substantially influence isotope ratios (Brooks et al., 2012; McGill et al., 2020). For the Snoqualmie River, MWE explained most of the variation in isotope ratios across seasons (Table 2), indicating that elevation-induced rainout is the greatest control on surface water isotope ratios. We use this observed elevation gradient in conjunction with seasonality in surface water isotopes to make inference on how various catchments across the basin contribute to river flow in the Snoqualmie River throughout the year.

## 4.2 | Seasonality in isotope ratios reflects hydrological processes

Seasonality in Snoqualmie basin surface water isotopes can be explained by both changes in the isotopic ratio of input precipitation

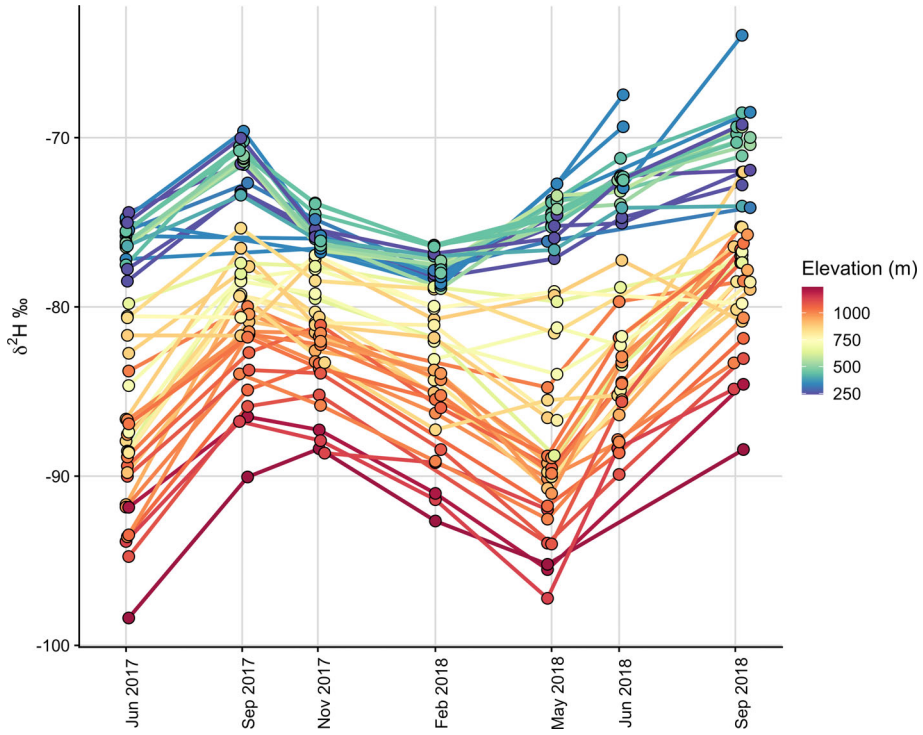


**FIGURE 5** The $\delta^2H$ values for all seasonal sites throughout the year. Colour indicates the MWE of the basin

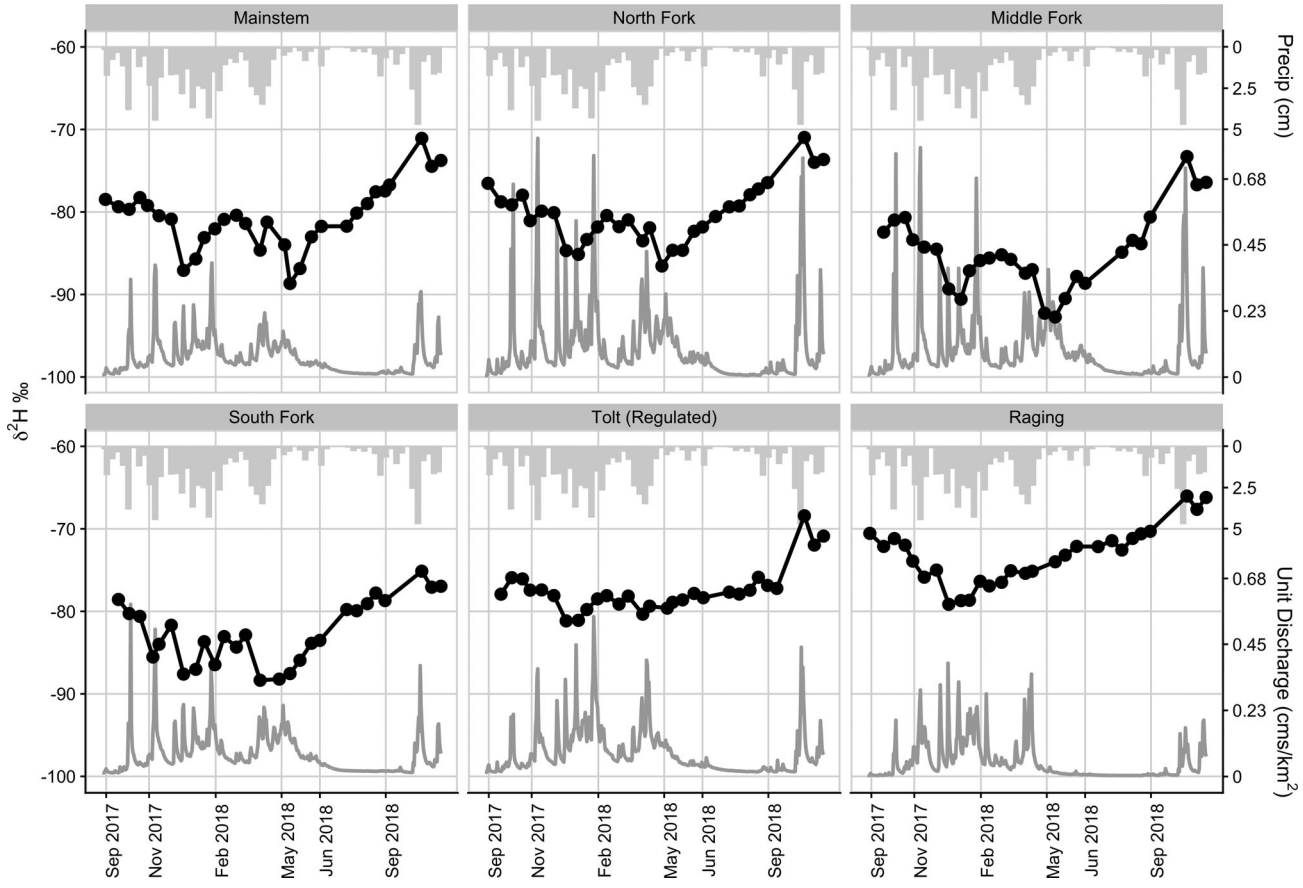


**FIGURE 6** Black lines are $\delta^2H$ values for biweekly samples collected at the mouth of the mainstem Snoqualmie and each major tributary over WY 2018. Dark grey lines along the bottom are daily streamflow hydrographs from nearby USGS gages, normalized by drainage area. Grey bars along the top are weekly averages of precipitation

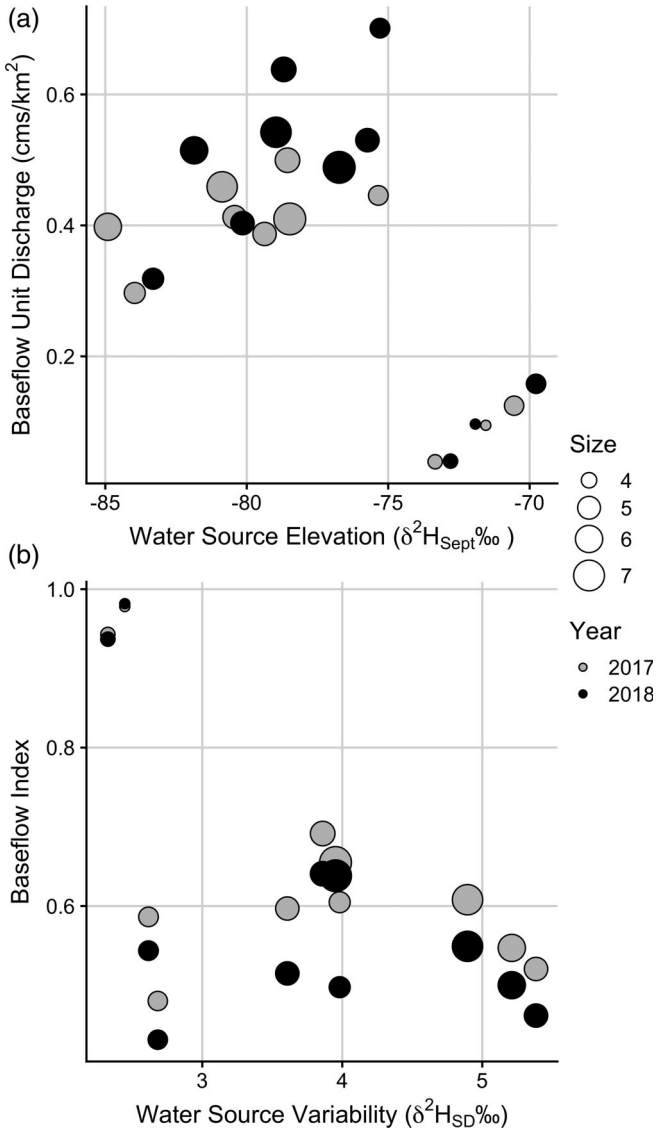


**FIGURE 7** Relationships between water source elevation and average unit discharge at baseflow (a) and water source variability and the baseflow index (b) for all streamflow gages within the basin. Points are coloured by year. Point size is related to the log watershed area for each site

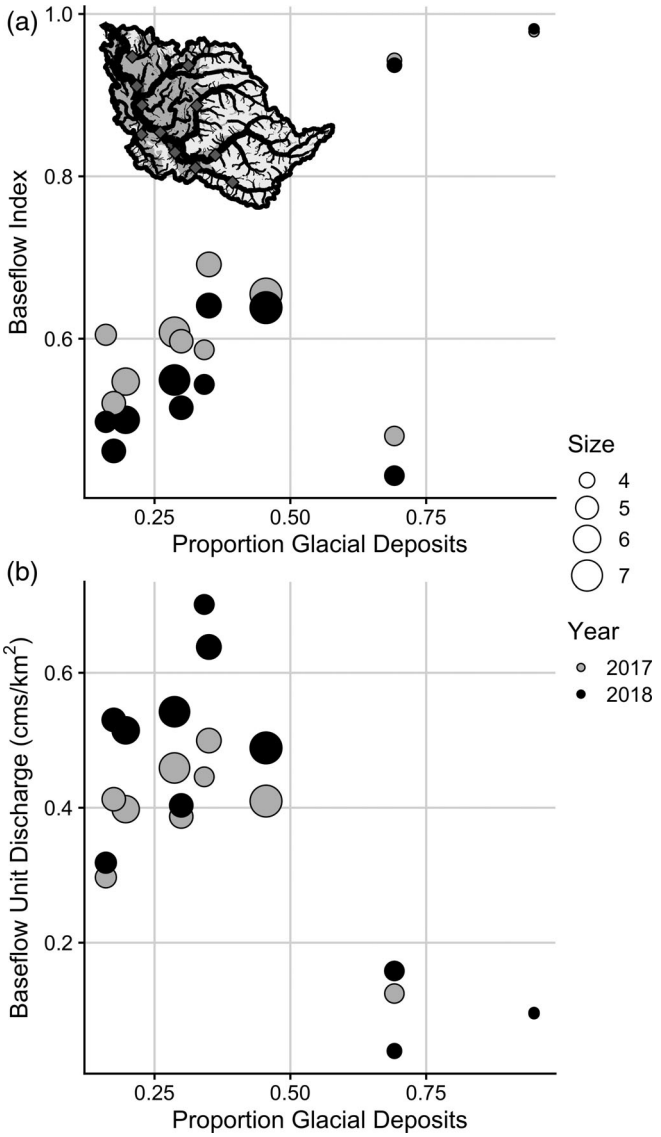


**FIGURE 8** Relationships between the proportion of glacial deposits within a watershed and the average unit discharge at baseflow (a) and baseflow index (b) for all streamflow gages within the basin. Points are coloured by year. Point size is related to the log watershed area for each site. The inset panel shows the Snoqualmie basin generalized geology (see Figure 1a for legend colours) and streamflow gage locations

entering the watershed and changes in contributing catchments. Within the Pacific Northwest, precipitation isotope ratios are highly variable, with little distinct seasonality (Brooks et al., 2012; Ersek et al., 2010; Nickolas et al., 2017). Therefore, the majority of variability in precipitation isotope ratios is storm specific. Although the exact causes of inter-storm variability are still uncertain, moisture source, temperature at condensation, air parcel trajectory, and the extent of the rainout process have all been shown to contribute to variability in precipitation isotope ratios (Berkelhammer et al., 2012; Ersek et al., 2010; McCabe-Glynn et al., 2016; Yoshimura et al., 2010). Biweekly timeseries data shows two large, basin-wide shifts in surface water isotope ratios, even in the regulated Tolt basin, that reflect variability in incoming precipitation isotopes (Figure 6). Both of these samples were taken on the rising limb of storms, where recent precipitation likely made up a larger percentage of streamflow. Large shifts in isotope ratios may therefore be the result of precipitation with isotopic ratios distinct from that of stream water entering the watershed and contributing to streamflow.

Isotope ratios from biweekly samples of major tributaries indicate that streamflow in fall and winter is predominately sourced from recent and lower elevation precipitation. In the humid Mediterranean climate western Washington experiences, winter precipitation begins in October and continues through March. This is typically the wettest and coldest time of the year (Figure 2). These conditions lead to snow accumulating in the high elevation mountains within the Snoqualmie

basin. Subsequently, lower elevation portions of watersheds are contributing more flow than higher elevation portions of the watersheds located in the transient (300–900 m) and seasonal (above 900 m) snow zones at this time, and the $\delta^2$H-MWE slope is shallowest (Jefferson, 2011; Figure 3; Table 2). High variability in early winter isotope ratios corresponding to changes in river discharge (Figure 6) suggest that most stream water is derived from recent precipitation in winter. Results from spatial modelling are consistent with this finding. In November and February samples, spatial autocorrelation not explained by MWE is low (Table 2; Figure 4). This occurs because precipitation amount, type, and isotopic signature are controlled by orographic processes that vary strongly with elevation, and during the wet winter a larger fraction of stream water derives directly from recent precipitation. Previous studies have found similar patterns, wherein during the winter rainy season and wetter-than-average summers the isotope ratios of surface water across Pacific Northwest river basins are consistent with recent precipitation, and differences in isotope ratios due to physical watershed characteristics are limited (Blumstock et al., 2015; Nickolas et al., 2017; Segura et al., 2019).

Lower surface water isotope ratios in high elevation sites and large $\delta^2$H-MWE slopes in May and June reflect the input of spring snowmelt to high elevation sites (Figures 4 and 6). According to SNOTEL data from across the basin, snowmelt in 2018 began in some locations as early as April and persisted until late June (Figure 2). However, SWE estimates at SNOTEL stations represent only a small subset of conditions within an area. SNOTEL stations are typically located at higher elevations and in areas that accumulate deeper snowpack than a majority of the surrounding landscape (Daly et al., 2000; Molotch & Bales, 2006). Therefore, the majority of realized snowmelt in the Snoqualmie basin likely began and ended earlier than SNOTEL data suggest. Slopes for $\delta^2$H-MWE relationships are largest in May and June (Table 2) and high elevation sampling sites show low isotope ratios compared to February (Figure 5). Snowmelt is typically $^{18}$O and $^{2}$H depleted relative to stream water and rain due to a combination of accumulating at high elevations and cold temperatures during fractionation (Beria et al., 2018). Furthermore, biweekly samples show a distinct drop in isotope ratios beginning in March that lasts until early June for the Mainstem, North Fork, Middle Fork, and South Fork, all tributaries with a substantial portion of the basin above the 900 m snowline (Figure 6).

Water isotope values within the regulated Tolt River were more stable over time than other tributaries similarly positioned in the watershed (Figure 6). The Tolt Reservoir is operated for flood control in winter, flow augmentation in summer, and provides drinking water to the City of Seattle year-round. The reservoir fills in late winter and spring, potentially holding back winter precipitation and high elevation snowmelt and releasing it during summer low flow. The isotope ratio of water within the Tolt Reservoir likely reflects the long-term average of river water input, which may explain the relatively flat isotope time series and lack of a discernable snowmelt signal in spring (Figure 6). Previous studies have found muted temporal isotopic variation below artificial impoundments and natural lakes, reflecting extended retention times and elevated river water mixing (Brooks et al., 2012; Kendall & Coplen, 2001; Trinh et al., 2017; Wassenaar et al., 2011). We did not observe d-excess values below 5‰, which indicated no appreciable evaporation within the reservoir (Figure 3).

## 4.3 | Catchment geology controls summer baseflow

We found that summer baseflow within the Snoqualmie basin was derived from low elevation sources. In our biweekly sampling, water isotope values slowly increased throughout the dry summer as flows decreased at outlets of the mainstem and major tributaries (Figure 6). The highest surface water isotope ratios were found in September. In Mediterranean climates without significant summer precipitation, water isotopes in precipitation infiltrating into mountain blocks with different residence times determine the isotopic composition of river water at baseflow. Shallow groundwater isotope ratios do not deviate significantly from the mean weighted annual composition of precipitation in temperate climates in areas without seasonal or spatial bias in recharge (Bowen et al., 2011; Clark & Fritz, 1997). As the vast majority of precipitation within the Snoqualmie basin falls in winter (Figure 2) and Pacific Northwest precipitation isotope ratios have little distinct seasonal pattern (Brooks et al., 2012; Ersek et al., 2010), a temporal bias in groundwater recharge is unlikely. The relatively high summer baseflow isotope ratios in the Snoqualmie basin therefore suggest a spatial bias in recharge towards lower elevation sources, given the strong $\delta^2$H-MWE relationship we observed in Figure 3.

Lower elevations of the Snoqualmie basin are dominated by a deep, permeable, productive glacial aquifer that we presume is the source of baseflow (Bethel, 2004; Turney et al., 1995). Glacial and interglacial deposits in the valley bottom contain several geohydrologic units, each with differing lithological and hydrologic characteristics that control aquifer potential. Deposits consist of a mix of unconsolidated gravel, sand, silt, clay, and peat and include geologic features of alluvium, recessional and advance outwash, till, ice-contact deposits, and confining beds (Bethel, 2004; Turney et al., 1995; Figure S2). Features such as alluvium and advance outwash consist of sand and gravel on average hundreds of feet thick and have better aquifer properties than units such as till or transitional beds (Turney et al., 1995). However, most glacial and interglacial deposits can form small but useable aquifers that may help sustain baseflow in summer months (Blumstock et al., 2015; Soulsby et al., 2004; Turney et al., 1995). In the Pacific Northwest more specifically, geology is critical in determining baseflow patterns. In Oregon, Nickolas et al. (2017) found that baseflow was sustained by permeable sandstone portions of the Marys River watershed, and Segura et al. (2019) found that during drought conditions water stored in deep seated earthflows, other Quaternary deposits, and porous volcanic bedrock supported baseflow. Furthermore, baseflow in the Oregon Cascades is supported by high elevation snowmelt that travels through extensive subsurface flow paths within highly porous and permeable young volcanic bedrock (Brooks et al., 2012; Tague et al., 2013; Tague & Grant, 2004). Such studies of streamflow show that Pacific Northwest rivers will

not respond uniformly to the same climate signal and illustrate the importance of subsurface geology in controlling baseflow.

The $^{18}O$ and $^{2}H$ enriched summer baseflow in the Snoqualmie also suggests that snowmelt does not recharge groundwater or contribute substantially to late summer baseflow, but rather comes out as a pulse during the spring freshet. We observed a distinct decrease in water isotope ratios during spring in the mainstem and major tributaries with area above 900 m (Jefferson, 2011), quickly followed by a continual increase in isotope ratios throughout summer (Figure 6; Table 2). Snowmelt enters and moves through the system in a quick pulse, and as the year progresses lower elevation water sources sustain streamflow. The upper portion of the Snoqualmie basin is covered by thin soil over impermeable bedrock lacking extensive fracture networks, meaning that rain and snowmelt are not retained in the mountains but are rapidly transmitted to the stream system (Bethel, 2004; Turney et al., 1995). Recharge in mountain areas such as the Snoqualmie basin can be permeability-limited rather than recharge-limited due to thin soils overlying low-permeability crystalline bedrock (Debose & Klungland, 1983; Flint et al., 2008; Goldin, 1973, 1992; Nelson, 1971). When the rate of snowmelt infiltration into soils exceeds percolation into bedrock, lateral flow occurs and water drains to streams or wetlands. Furthermore, in the Pacific Northwest, spring snowmelt may substantially exceed unsaturated zone storage capacity due to high antecedent soil moisture from winter rains (Blankinship et al., 2014). Therefore, upper elevation bedrock is not an important source of runoff control and groundwater storage.

Hydrologic evidence supports the assertion that low elevation glacial deposits are the main source of summer baseflow. Unit discharge for baseflow increased when water originated from lower elevation (Figure 7b), supporting the idea that baseflow was sourced from a glacial aquifer within the Snoqualmie valley. Interestingly, three watersheds with mean elevations below 550 m, including the Raging River, had the smallest unit discharge values despite having a low water source elevation, high baseflow index and a large proportion of glacial deposits (Figures 7 and 8). These watersheds may have these unexpected attributes because less precipitation is entering the catchment or because their subsurface catchment is smaller than their topography delineated catchment (Nickolas et al., 2017). In addition, groundwater upwelling generally occurs at breaks in the landscape (Neff et al., 2020), and all these basins are below the break related to the Snoqualmie falls potentially limiting groundwater discharge points. A mass balance calculation using river discharge data also suggests that during summer, proportionally more water enters the basin from low elevation sources such as mainstem tributaries.

For all sites except the Raging River, as the proportion of glacial deposits within a catchment increases, the baseflow index increases linearly (Figure 8) meaning groundwater comprises a larger percentage of annual streamflow. The lack of a relationship between water source variability and baseflow index is surprising (Figure 7). We expect groundwater to have a relatively constant isotope ratio through time (Clark & Fritz, 1997), and therefore anticipate that sites dominated by groundwater have a low water source variability. We hypothesize that the weak pattern is partially due to our limited temporal sampling, which captures events on long time scales (e.g., snowmelt) better than on short timescales (e.g., storm driven events). Therefore, our metric of water source variability is correlated with elevation and snowmelt and may not capture the true water source variability for a site like the Raging River, which is a flashy system that lacks snowmelt.

Alternative explanations for $^{18}O$ and $^{2}H$ enriched summer baseflow, such as enriched precipitation falling in summer or displacement of evaporated soil water with an enriched isotopic composition, are unlikely. Very little rain falls in summer within the Snoqualmie basin; stream discharge response to summer precipitation is limited (Figure 2), likely because dry soils and plant transpiration adsorb and utilize these small summer events. In addition, evaporatively enriched soil water was not the cause of the increase in stream water isotope values as seen in some other studies (Peralta-Tapia et al., 2015; Sprenger et al., 2017; Tetzlaff et al., 2015), because September samples had a similar d-excess as June samples. Brooks et al. (2010) found tightly bound soil water with an evaporatively enriched isotopic signal remained stationary throughout summer unless utilized by plants, and mobile water without an evaporated signal contributed to streamflow in a similar Mediterranean climate. Good et al. (2015) suggested that globally this process is more widespread than previously thought. The observed isotopic increase in baseflow was therefore likely due to a decrease in elevation of the water origin, indicating that $^{18}O$ and $^{2}H$ enriched lower-elevation groundwater is contributing more to streamflow in late summer. Additionally, residual snowmelt, which may be present in June, did not sustain streamflow into September.

## 4.4 | Caveats and limitations

Our ability to generalize results is limited by our sampling design and dataset. Our sampling design involved intensive temporal and spatial sampling over June and September 2017 and the 2018 water year. The coupling of widespread and frequent water sampling provided information about geologic and climatic controls on the spatial and temporal variability of water sources relevant to management. Given that our study only spanned a single year, our results may be a reflection of specific conditions during the 2018 water year. However, as 2018 was a relatively average year in terms of temperature and precipitation (Figure S3), this seems unlikely. Precipitation samples were not collected within the Snoqualmie basin due to logistical restrictions, although we obtained precipitation samples from a nearby location.

## 4.5 | Climate and management implications

A critical challenge for resource managers seeking to prioritize restoration or research actions is in identifying streamflow sensitivity to climate change. Our results show that in the Snoqualmie basin, summer streamflow is sustained primarily by groundwater recharged by low elevation precipitation, and snowmelt does not substantially contribute to summer streamflow. This suggests that the Snoqualmie River

may be less sensitive to predicted warming than Pacific Northwest rivers that rely on snow or glacial melt to sustain summer streamflow (Brooks et al., 2012; Riedel & Larrabee, 2016). However, it is important to note that although groundwater discharge may remain constant, warmer air temperatures could lead to warmer water temperatures and a reduction in baseflow discharge due to increased evaporation and evapotranspiration. Furthermore, groundwater likely integrates several years of storage; amount of storage and timing of release to the stream are key considerations for drought resiliency. Although several studies have highlighted the role of underlying geology in controlling hydrologic responses to climate change (Mayer & Naman, 2011; Tague & Grant, 2004, 2009), future streamflow predictions for Puget Sound continue to focus predominately on climate mediated changes in snowpack regimes (Elsner et al., 2010; Mantua et al., 2010; Wu et al., 2012). An increased focus on basin-scale attributes that impact timing and magnitude groundwater discharge to rivers could improve future streamflow predictions (Tague et al., 2013).

Recognizing that subsurface geology plays a major role in controlling the hydrology of the Snoqualmie River can be used to advise management decisions relating to restoring floodplain functions that recharge aquifers. Understanding major groundwater recharge areas may enable managers to target restoration actions such as placing engineered logjams or reintroducing beavers in areas underlain by permeable glacial deposits where recharge is greatest (Abbe & Brooks, 2013; Pollock et al., 2014). Similarly, by combining climate predictions with our water source estimates we can estimate areas of the basin and times of year that will undergo the greatest shifts in streamflow timing and magnitude. For example, Figure 6 illustrates that recent precipitation from incoming storms can dominate streamflow across the Snoqualmie River. Climate models predict more intense and frequent winter storms, which have the potential to cause flooding across all areas of the basin. Impacts from flooding could be particularly severe in the Raging River due to its flashy hydrology and low elevation. Several species of Pacific Salmon spawn in the Raging River and flooding here may negatively impact egg-to-fry survival rates (Isaak et al., 2012; Mantua et al., 2010). Resource managers may therefore decide to preemptively focus management efforts such as wetland restoration and riparian planting within this and other low-elevation tributaries to provide fish habitat complexity and mitigate flood risk.

## 4.6 | Conclusions

In this study we used surface water isotopic variation to develop a conceptual model of streamflow provenance for the Snoqualmie River. Stable isotope ratios in river water related strongly to elevation throughout the year, however, seasonal variation in isotope ratios was present and reflected hydrologic processes. Low isotope values in spring reflected the input of snowmelt into the river. High baseflow isotope values suggest that groundwater is sourced from low elevation glacial deposits and recharged by winter precipitation. Our results illustrate that stable isotopes of surface water can be used to understand water source dynamics and provide insights into management strategies across the Snoqualmie River basin. Future research should integrate water isotopes with empirical measures of groundwater, stream temperature, and processed based hydrological modelling to better understand how climate induced change will impact stream temperature and flow. Continued monitoring of the Snoqualmie mainstem and major tributary stable isotopes would provide a valuable understanding of how water sources shift over years of fluctuating climate and snowpack.

## ACKNOWLEDGEMENTS

We thank Aimee Fullerton, Amy Marsha, and the many volunteers for helping collect water samples, Seattle City Light for granting access to the Tolt River, and Dr. Gordon Holtgrieve and two anonymous reviewers for suggestions that improved the manuscript. This research was funded by a Department of the Interior Northwest Climate Adaptation Science Center graduate fellowship awarded to Lillian McGill. This material is based upon work supported by the National Science Foundation Graduate Research Fellowship under Grant No. DGE-1762114. Any opinion, findings, and conclusions or recommendations expressed in this material are those of the authors and do not necessarily reflect the views of the National Science Foundation. This manuscript has been subjected to Agency review and has been approved for publication. The views expressed in this paper are those of the author(s) and do not necessarily reflect the views or policies of the U.S. Environmental Protection Agency. Mention of trade names or commercial products does not constitute endorsement or recommendation for use.

## DATA AVAILABILITY STATEMENT

The data that support the findings of this study are openly available in the EPA ScienceHub at http://doi.org/10.23719/1520140.

## ORCID

*Lillian M. McGill* https://orcid.org/0000-0003-2722-2917
*J. Renée Brooks* https://orcid.org/0000-0002-5008-9774

## REFERENCES

Abbe, T., & Brooks, A. (2011, 2013). Geomorphic. In A. Simon, S. J. Bennett, & J. M. Castro (Eds.), *Engineering, and ecological considerations when using wood in river restoration*. *Geophysical monograph series* (pp. 419–451). American Geophysical Union.

Araguas-Araguas, L., Froehlich, K., & Rozanski, K. (2000). Deuterium and oxygen-18 isotope composition of precipitation and atmospheric moisture. *Hydrological Processes*, *14*, 1341–1355.

Beck, H. E., van Dijk, A. I. J. M., Miralles, D. G., de Jeu, R. A. M., Sampurno Bruijnz, L. A., McVicar, T. R., & Schellekens, J. (2013). Global patterns in base flow index and recession based on streamflow observations from 3394 catchments. *Water Resources Research*, *49*, 7843–7863.

Beria, H., Larsen, J. R., Ceperley, N. C., Michelon, A., Vennemann, T., & Schaefli, B. (2018). Understanding snow hydrological processes through the lens of stable water isotopes. *WIREs Water*, *5*, 1–23.

Berkelhammer, M., Stott, L., Yoshimura, K., Johnson, K., & Sinha, A. (2012). Synoptic and mesoscale controls on the isotopic composition of precipitation in the western United States. *Climate Dynamics*, *38*, 433–454.

Bethel, J. (2004). *An overview of the geology and geomorphology of the Snoqualmie River watershed*. King County Water and Land Resources Division, Snoqualmie Watershed Team.

Blankinship, J. C., Meadows, M. W., Lucas, R. G., & Hart, S. C. (2014). Snowmelt timing alters shallow but not deep soil moisture in the Sierra Nevada. *Water Resources Research*, *50*, 1448–1456.

Blumstock, M., Tetzlaff, D., Malcolm, I. A., Nuetzmann, G., & Soulsby, C. (2015). Baseflow dynamics: Multi-tracer surveys to assess variable groundwater contributions to montane streams under low flows. *Journal of Hydrology*, *527*, 1021–1033.

Bowen, G. J., & Good, S. P. (2015). Incorporating water isoscapes in hydrological and water resource investigations. *Wiley Interdisciplinary Reviews: Water*, *2*, 107–119.

Bowen, G. J., Kennedy, C. D., Liu, Z., & Stalker, J. (2011). Water balance model for mean annual hydrogen and oxygen isotope distributions in surface waters of the contiguous United States. *Journal of Geophysical Research*, *116*, G04011.

Brennan, S. R., Torgersen, C. E., Hollenbeck, J. P., Fernandez, D. P., Jensen, C. K., & Schindler, D. E. (2016). Dendritic network models: Improving isoscapes and quantifying influence of landscape and in-stream processes on strontium isotopes in rivers. *Geophysical Research Letters*, *43*, 5043–5051.

Brooks, J. R., Barnard, H. R., Coulombe, R., & McDonnell, J. J. (2010). Ecohydrologic separation of water between trees and streams in a Mediterranean climate. *Nature Geoscience*, *3*, 100–104.

Brooks, J. R., Wigington, P. J., Phillips, D. L., Comeleo, R., & Coulombe, R. (2012). Willamette River Basin surface water isoscape ($\delta^{18}O$ and $\delta^{2}H$): Temporal changes of source water within the river. *Ecosphere*, *3*, 39.

Buffington, J. M., Woodsmith, R. D., Booth, D. B., & Montgomery, D. R. (2003). Fluvial processes in Puget Sound Rivers and the Pacific Northwest. In D. R. Montgomery, S. Bolton, D. B. Booth, & L. Wall (Eds.), 2003 *Restoration of Puget Sound Rivers* (p. 505). University of Washington Press.

Clark, I. D., & Fritz, P. (1997). *Environmental isotopes in hydrogeology*. CRC Press/Lewis Publishers 1997.

Cressie, N. (1993). *Statistics for spatial data* (p. 900). John Wiley.

Daly, S. F., Davis, R. E., Ochs, E., & Pangburn, T. (2000). An approach to spatially distributed snow modelling of the Sacramento and San Joaquin basins, California. *Hydrological Processes*, *14*, 3257–3271.

Dansgaard, W. (1964). Stable isotopes in precipitation. *Tellus*, *16*, 436–468.

Debose, A., & M.W. Klungland. (1983). *Soil survey of Snohomish County area*, Washington, DC. US Department of Agriculture, Soil Conservation Service.

Dutton, A., Wilkinson, B. H., Welker, J. M., Bowen, G. J., & Lohmann, K. C. (2005). Spatial distribution and seasonal variation in $^{18}O/^{16}O$ of modern precipitation and river water across the conterminous USA. *Hydrological Processes*, *19*, 4121–4146.

Elsner, M. M., Cuo, L., Voisin, N., Deems, J. S., Hamlet, A. F., Vano, J. A., Mickelson, K. E. B., Lee, S.-Y., & Lettenmaier, D. P. (2010). Implications of 21st century climate change for the hydrology of Washington State. *Climatic Change*, *102*, 225–260.

Ersek, V., Mix, A. C., & Clark, P. U. (2010). Variations of $\delta^{18}O$ in rainwater from southwestern Oregon. *Journal of Geophysical Research*, *115*, D09109.

Flint, A. L., Flint, L. E., & Dettinger, M. D. (2008). Modeling soil moisture processes and recharge under a melting snowpack. *Vadose Zone Journal*, *7*, 350–357.

Floriancic, M. G., Fischer, B. M. C., Molnar, P., Kirchner, J. W., & Meerveld, I. H. J. (2019). Spatial variability in specific discharge and streamwater chemistry during low flows: Results from snapshot sampling campaigns in eleven Swiss catchments. *Hydrological Processes*, *33*, 2847–2866.

Frizzell, V. A., Tabor, R. W., Booth, D. B., Ort, K. M., & Waitt, R. B. (1984). *Preliminary geologic map of the Snoqualmie Pass 1:100,000 quadrangle*, Washington. U.S. Geological Survey Open-File Report 84-693, p. 43.

Gat, J. R. (1996). Oxygen and hydrogen isotopes in the hydrologic cycle. *Annual Review of Earth and Planetary Sciences*, *24*, 225–262.

Gesch, D. B., Evans, G. A., Oimoen, M. J., & Arundel, S. (2018). *The National Elevation Dataset* (pp. 83–100). American Society for Photogrammetry and Remote Sensing.

Goldin, A. (1973). *Soil survey of King County area, Washington*. US Department of Agriculture, Soil Conservation Service, Washington, DC.

Goldin, A. (1992). *Soil survey of Whatcom County area, Washington*. US Department of Agriculture, Soil Conservation Service, Washington, DC.

Good, S. P., Noone, D., & Bowen, G. (2015). Hydrologic connectivity constrains partitioning of global terrestrial water fluxes. *Science*, *349*, 175–177.

Hamlet, A. F., Lee, S.-Y., Mickelson, K. E. B., & Elsner, M. M. (2010). Effects of projected climate change on energy supply and demand in the Pacific Northwest and Washington State. *Climatic Change*, *102*, 103–128.

Hill, R. A., Weber, M. H., Liebowitz, S. G., Olsen, A. R., & Thornbrugh, D. J. (2015). The Stream-Catchment (StreamCat) Dataset: A database of watershed metrics for the conterminous United States. *Journal of the American Water Resources Association*, *51*(1), 120–128.

Ingraham, N. L., & Taylor, B. E. (1986). Hydrogen isotope study of large-scale meteoric water transport in Northern California and Nevada. *Journal of Hydrology*, *85*, 183–197.

Ingraham, N. L., & Taylor, B. E. (1991). Light stable isotope systematics of large-scale hydrologic regimes in California and Nevada. *Water Resources Research*, *27*, 77–90.

Isaak, D. J., Wollrab, S., Horan, D., & Chandler, G. (2012). Climate change effects on stream and river temperatures across the northwest U.S. from 1980–2009 and implications for salmonid fishes. *Climatic Change*, *113*, 499–524.

Jaeger, W. K., Plantinga, A. J., Chang, H., Dello, K., Grant, G., Hulse, D., McDonnell, J. J., Lancaster, S., Moradkhani, H., Morzillo, A. T., Mote, P., Nolin, A., Santelmann, M., & Wu, J. (2013). Toward a formal definition of water scarcity in natural-human systems. *Water Resources Research*, *49*, 4506–4517.

Jefferson, A. J. (2011). Seasonal versus transient snow and the elevation dependence of climate sensitivity in maritime mountainous regions. *Geophysical Research Letters*, *38*, L16402.

Kendall, C., & Coplen, T. B. (2001). Distribution of oxygen-18 and deuterium in river waters across the United States. *Hydrological Processes*, *15*, 1363–1393.

Kennard, M. J., Mackay, S. J., Pusey, B. J., Olden, J. D., & Marsh, N. (2009). Quantifying uncertainty in estimation of hydrologic metrics for ecohydrological studies. *River Research and Applications*, *26*(2), 137–156.

Koffler, D., Gauster, T., & Laaha, G. (2013). *lfstat: Calculation of low flow statistics for daily stream flow data*. R package version 0.9.4. Retrieved from https://cran.rproject.org/web/packages/lfstat/index.html

Lechler, A. R., & Niemi, N. A. (2011). Controls on the spatial variability of modern meteoric $^{18}O$: Empirical constraints from the Western U.S. and East Asia and implications for stable isotope studies. *American Journal of Science*, *311*, 664–700.

Mantua, N., Tohver, I., & Hamlet, A. (2010). Climate change impacts on streamflow extremes and summertime stream temperature and their possible consequences for freshwater salmon habitat in Washington State. *Climatic Change*, *102*, 187–223.

Mayer, T. D., & Naman, S. W. (2011). Streamflow response to climate as influenced by geology and elevation. *Journal of the American Water Resources Association*, *47*(4), 724–738.

McCabe-Glynn, S., Johnston, K. R., Strong, C., Zou, Y., Yu, J., Sellars, S., & Welker, J. M. (2016). Isotopic signature of extreme precipitation events in the western U.S. and associated phases of Arctic and tropical climate modes. *Journal of Geophysical Research: Atmospheres*, *121*, 8913–8924.

McGill, L. M., Steel, E. A., Brooks, J. R., Edwards, R. T., & Fullerton, A. F. (2020). Elevation and spatial structure explain most surface water isotopic variation across five Pacific Coast basins. *Journal of Hydrology*, *583*, 124610.

McGuire, K. J., Torgersen, C. E., Likens, G. E., Buso, D. C., Lowe, W. H., & Bailey, S. W. (2014). Network analysis reveals multiscale controls on streamwater chemistry. *Proceedings of the National Academy of Sciences of the United States of America*, *111*, 7030–7035.

Molotch, N. P., & Bales, R. C. (2006). SNOTEL representativeness in the Rio Grande headwaters on the basis of physiographics and remotely sensed snow cover persistence. *Hydrological Processes*, *20*, 723–739.

Neff, B., Rosenberry, D. O., Leibowitz, S. G., Mushet, D. M., Golden, H. E., Rains, M. C., Brook, J. R., & Lane, C. R. (2020). A hydrologic landscapes perspective on groundwater connectivity of depressional wetlands. *Water*, *12*, 50.

Nelson, L. M. (1971). *Sediment transport by streams in the Snohomish River basin, Washington: October 1967 – June 1969*. USGS Open-File Report 71-213.

Nickolas, L. B., Segura, C., & Brooks, J. R. (2017). The influence of lithology on surface water sources. *Hydrological Processes*, *31*, 1913–1925.

Nolin, A. W., & Daly, C. (2006). Mapping "at risk" snow in the Pacific Northwest. *Journal of Hydrometeorology*, *7*, 1164–1171.

Olden, J. D., Kennard, M. J., & Pusey, B. J. (2011). A framework for hydrologic classification with a review of methodologies and applications in ecohydrology. *Ecohydrology*, *5*, 503–518.

Peralta-Tapia, A., Sponseller, R. A., Tetzlaff, D., Soulsby, C., & Laudon, H. (2015). Connecting precipitation inputs and soil flow pathways to stream water in contrasting boreal catchments. *Hydrological Processes*, *29*, 3546–3555.

Peterson, E. E., & Ver Hoef, J. M. (2010). A mixed-model moving-average approach to geostatistical modeling in stream networks. *Ecology*, *91*, 451–644.

Peterson, E. E., & Ver Hoef, J. M. (2014). An ArcGIS toolset used to calculate the spatial information needed to fit spatial statistical models to stream network data. *Journal of Statistical Software*, *56*(2), 1–17.

Pollock, M. M., Beechie, T. J., Wheaton, J. M., Jordan, C. E., Bouwes, N., Weber, N., & Volk, C. (2014). Using beaver dams to restore incised stream ecosystems. *BioScience*, *64*, 279–290.

Reidy Liermann, C. A., Olden, J. D., Beechie, T. J., Kennard, M. J., Skidmore, P. B., Konrad, C. P., & Imaki, H. (2011). Hydrogeomorphic classification of Washington state rivers to support emerging environmental flow management strategies. *River Research and Applications*, *28*, 1340–1358.

Riedel, J. L., & Larrabee, M. A. (2016). Impact of recent glacial recession on summer streamflow in the Skagit River. *Northwest Science*, *90*, 5–22.

Ruhi, A., Messager, M. L., & Olden, J. D. (2018). Tracking the pulse of the Earth's fresh waters. *Nature Sustainability*, *1*, 198–203.

Safeeq, M., Grant, G. E., Lewis, S. L., Kramer, M. G., & Staab, B. (2014). A hydrogeologic framework for characterizing summer streamflow sensitivity to climate warming in the Pacific Northwest, USA. *Hydrological and Earth Systems Sciences*, *18*, 3693–3710.

Safeeq, M., Grant, G. E., Lewis, S. L., & Tague, C. L. (2013). Coupling snowpack and groundwater dynamics to interpret historical streamflow trends in the western United States. *Hydrological Processes*, *27*, 655–668.

Safeeq, M., Mauger, G. S., Grant, G. E., Arismendi, I., Hamlet, A. F., & Lee, S. (2014). Comparing large-scale hydrological model predictions with observed streamflow in the Pacific Northwest: Effects of climate and groundwater. *Journal of Hydrometerology*, *15*(6), 2501–2521.

Segura, C., Noone, D., Warren, D., Jones, J. A., Tenny, J., & Ganio, L. M. (2019). Climate, landforms, and geology affect baseflow sources in a mountain catchment. *Water Resources Research*, *55*, 5238–5254.

Smakhtin, V. U. (2001). Low flow hydrology: A review. *Journal of Hydrology*, *240*, 147–186.

Soulsby, C., Rodgers, P. J., Petry, J., Hannah, D. M., Malcolm, I. A., & Dunn, S. M. (2004). Using tracers to upscale flow path understanding in mesoscale mountainous catchments: Two examples from Scotland. *Journal of Hydrology*, *291*, 174–196.

Sprenger, M., Tetzlaff, D., Tunaley, C., Dick, J. M., & Soulsby, C. (2017). Evaporation fractionation in a peatland drainage network affects stream water isotope composition. *Water Resources Research*, *53*, 851–866.

Steel, A. E., Sowder, C., & Peterson, E. E. (2016). Spatial and temporal variation of water temperature regimes on the Snoqualmie River network. *Journal of the American Water Resources Association*, *52*, 769–787.

Stewart, I. T., Cayan, D. R., & Dettinger, M. D. (2005). Changes toward earlier streamflow timing across Western North America. *Journal of Climate*, *18*, 1136–1155.

Tabor, R. W., Frizzell, V. A., Booth, D. B., Waitt, R. B., Whetten, J.T., & Zartman, R.E. (1993). *Geologic map of the Skykomish River 30- by 60-minute quadrangle, Washington*. U.S. Geological Survey Miscellaneous Investigations Series Map 1-1963, p. 42.

Tague, C., & Grant, G. E. (2004). A geological framework for interpreting the low-flow regimes of Cascade streams, Willamette River Basin, Oregon. *Water Resources Research*, *40*, W04303.

Tague, C., & Grant, G. E. (2009). Groundwater dynamics mediate low-flow response to global warming in snow dominated alpine regions. *Water Resources Research*, *45*, W07421.

Tague, C. L., Choate, J. S., & Grant, G. (2013). Parameterizing sub-surface drainage with geology to improve modeling streamflow responses to climate in data limited environments. *Hydrology and Earth System Sciences*, *17*, 341–354.

Tetzlaff, D., Buttle, J., Carey, S. K., van Huijgevoort, M., Laudon, H., McNamara, J. P., Mitchell, C. P. J., Spence, C., Gabor, R. S., & Soulsby, C. (2015). A preliminary assessment of water partitioning and ecohydrological coupling in northern headwaters using stable isotopes and conceptual runoff models. *Hydrological Processes*, *29*, 5153–5173.

Trinh, D. A., Luu, M. T. N., & Le, Q. T. P. (2017). Use of stable isotopes to understand run-off generation processes in the Red River Delta. *Hydrological Processes*, *31*, 3827–3843.

Turney, G.L., S.C. Kahle, & N.P. Dion. (1995). *Geohydrology and groundwater quality of east King County, Washington*. Prepared in cooperation with Seattle-King County Department of Health, Tacoma, Washington. US Geological Survey, Water Resources Investigations Report 94-4082, Washington, DC.

U.S. Geological Survey. (2001). *National Water Information System data available on the World Wide Web (Water Data for the Nation)*. Retrieved from http://waterdata.usgs.gov/nwis/

USDA Natural Resources Conservation Service. (2020). *SNOwpack TELemetry Network (SNOTEL)*. Ag Data Commons, Retrieved from https://data.nal.usda.gov/dataset/snowpack-telemetry-network-snotel

Vano, J. A., Nijssen, B., & Lettenmaier, D. P. (2015). Seasonal hydrologic responses to climate change in the Pacific Northwest. *Water Resources Research*, *51*, 1959–1976.

Vano, J. A., Voisin, N., Cuo, L., Hamlet, A. F., Elsner, M. M., Palmer, R. N., Polebitski, A., & Lettenmaier, D. P. (2010). Climate change impacts on water management in the Puget Sound region, Washington State, USA. *Climatic Change*, *102*(1–2), 261–286.

Ver Hoef, J. M., & Peterson, E. E. (2010). A moving average approach to spatial statistical models of stream networks. *Journal of the American Statistical Association*, *489*, 6–18.

Ver Hoef, J. M., Peterson, E. E., Clifford, D., & Shah, R. (2014). SSN: An R package for spatial statistical modeling on stream networks. *Journal of Statistical Software*, *56*(3), 1–45.

Ver Hoef, J. M., Peterson, E. E., & Theobald, D. (2006). Spatial statistical models that use flow and stream distance. *Environmental and Ecological Statistics*, *12*, 449–464.

Wassenaar, L. I., Athanasopoulos, P., & Hendry, M. J. (2011). Isotope hydrology of precipitation, surface and ground waters in the Okanagan Valley, British Columbia, Canada. *Journal of Hydrology*, *411*, 37–48.

Wenger, S. J., Luce, C. H., Hamlet, A. F., Isaak, D. J., & Neville, H. M. (2010). Macroscale hydrologic modeling of ecologically relevant flow metrics. *Water Resources Research*, *46*, W09513.

Wigington, P. J., Leibowitz, S. G., Comeleo, R. L., & Ebersole, J. L. (2013). Oregon hydrologic landscapes: A classification framework 1: Oregon hydrologic landscapes: A classification framework. *Journal of the American Water Resources Association*, *49*, 163–182.

Wolock, D. M., Winter, T. C., & McMahon, G. (2004). Delineation and evaluation of hydrologic-landscape regions in the United States using geographic information system tools and multivariate statistical analyses. *Environmental Management*, *34*, S71–S88.

Wu, H., Kimball, J. S., Elsner, M. M., Mantua, N., Adler, R. F., & Stanford, J. (2012). Projected climate change impacts on the hydrology and temperature of Pacific Northwest rivers. *Water Resources Research*, *48*, W11530.

Yonge, C. J., Goldenberg, L., & Krouse, H. R. (1989). An isotope study of water bodies along a traverse of southwestern Canada. *Journal of Hydrology*, *106*, 245–255.

Yoshimura, K., Kanamitsu, M., & Dettinger, M. (2010). Regional downscaling for stable water isotopes: A case study of an atmospheric river event. *Journal of Geophysical Research*, *115*, D18114.

Yount, J. C., & Gower, H. D. (1991). *Bedrock geologic map of the Seattle 30-by 60-minute quadrangle, Washington*. U.S. Geological Survey Open-File Report 91-147, p. 37.

Zimmerman, D. L., & Ver Hoef, J. M. (2017). The torgegram for fluvial variography: Characterizing spatial dependence on stream networks. *Journal of Computational and Graphical Statistics*, *26*, 253–264.

## SUPPORTING INFORMATION

Additional supporting information may be found online in the Supporting Information section at the end of this article.

**How to cite this article:** McGill LM, Brooks JR, Steel EA. Spatiotemporal dynamics of water sources in a mountain river basin inferred through $\delta^2H$ and $\delta^{18}O$ of water. *Hydrological Processes*. 2021;35:e14063. https://doi.org/10.1002/hyp.14063